



LUND UNIVERSITY

Kinetics and mechanism for reduction of Pt(IV) anticancer model compounds by Se-methyl L-selenocysteine. Comparison with L-selenomethionine.

Liu, Chunli; Xu, Liyao; Tian, Hongwu; Yao, Haiping; Elding, Lars Ivar; Shi, Tiesheng

Published in:
Journal of Molecular Liquids

DOI:
[10.1016/j.molliq.2018.09.056](https://doi.org/10.1016/j.molliq.2018.09.056)

2018

Document Version:
Publisher's PDF, also known as Version of record

[Link to publication](#)

Citation for published version (APA):
Liu, C., Xu, L., Tian, H., Yao, H., Elding, L. I., & Shi, T. (2018). Kinetics and mechanism for reduction of Pt(IV) anticancer model compounds by Se-methyl L-selenocysteine. Comparison with L-selenomethionine. *Journal of Molecular Liquids*, 2018(271), 838-843. <https://doi.org/10.1016/j.molliq.2018.09.056>

Total number of authors:
6

General rights

Unless other specific re-use rights are stated the following general rights apply:
Copyright and moral rights for the publications made accessible in the public portal are retained by the authors and/or other copyright owners and it is a condition of accessing publications that users recognise and abide by the legal requirements associated with these rights.

- Users may download and print one copy of any publication from the public portal for the purpose of private study or research.
- You may not further distribute the material or use it for any profit-making activity or commercial gain
- You may freely distribute the URL identifying the publication in the public portal

Read more about Creative commons licenses: <https://creativecommons.org/licenses/>

Take down policy

If you believe that this document breaches copyright please contact us providing details, and we will remove access to the work immediately and investigate your claim.

LUND UNIVERSITY

PO Box 117
221 00 Lund
+46 46-222 00 00



Kinetics and mechanism for reduction of Pt(IV) anticancer model compounds by Se-methyl L-selenocysteine. Comparison with L-selenomethionine

Chunli Liu ^{a,*}, Liyao Xu ^b, Hongwu Tian ^b, Haiping Yao ^b, Lars I. Elding ^c, Tiesheng Shi ^{a,*}

^a College of Chemistry, Chemical Engineering and Materials Science, Zaozhuang University, Zaozhuang 277160, Shandong Province, People's Republic of China

^b College of Chemistry and Environmental Science, and the MOE Key Laboratory of Medicinal Chemistry and Molecular Diagnostics, Hebei University, Baoding 071002, Hebei Province, People's Republic of China

^c Center for Analysis and Synthesis, Department of Chemistry, Lund University, PO Box 124, SE 221 00, Lund, Sweden

ARTICLE INFO

Article history:

Received 29 July 2018

Received in revised form 8 September 2018

Accepted 10 September 2018

Available online 12 September 2018

ABSTRACT

Se-methyl L-selenocysteine (MeSeCys) is one of the major organic selenium compounds acquired from the diet by human beings. It has been shown to have anticancer activity and cancer prevention functions. However, its antioxidant activity, largely related to its biological function, has not been well characterized so far. We here report a stopped-flow kinetic study of the reduction of the Pt(IV) anticancer model compounds *trans*-[PtX₂(CN)₄]²⁻ (X = Cl; Br) by MeSeCys in a wide pH range. Overall second-order kinetics is established for the redox reactions, and spectrophotometric titrations indicate a 1:1 reaction stoichiometry. The MeSeCys is oxidized to its selenoxide form, as identified by high-resolution mass spectra. The proposed reaction mechanism involves parallel attack on one of the *trans*-coordinated halides of the Pt(IV) complexes by the selenium atom of the various MeSeCys protolytic species. Rate constants for the rate determining steps as well as the pK_a values of the various protolytic species of MeSeCys have been determined at 25.0 °C and 1.0 M ionic strength. A bridged two-electron transfer mechanism for the rate-determining steps is supported by rapid-scan spectra, activation parameters, and by the much larger reaction rate of [PtBr₂(CN)₄]²⁻ compared to [PtCl₂(CN)₄]²⁻. The experiments indicate that the reduction of [PtX₂(CN)₄]²⁻ by MeSeCys proceeds via a similar reaction mechanism as L-selenomethionine (SeMet) studied previously. However, there is a large reactivity difference between these two selenium compounds, as a matter of fact the largest one observed so far when compared to other redox systems. It differs between the various protolytic species of MeSeCys and SeMet. The different reactivity of MeSeCys and SeMet in the reduction of various biologically relevant oxidants might account for their disparate efficacies as anticancer agents.

© 2018 Elsevier B.V. All rights reserved.

1. Introduction

The trace element selenium is essential to human health in prevention of a number of degenerative conditions, as established during the last few decades [1–16]. These conditions include cancer, thyroid function, aging, infertility, infections, and inflammatory, cardiovascular and neurological diseases. Selenium is acquired by human beings through the diet and involves several compounds: L-selenomethionine (SeMet), Se-methyl L-selenocysteine (MeSeCys), L-selenocysteine, selenite and selenate [17–20]. Commercially available selenium supplements also contain these forms. It has been demonstrated that SeMet and MeSeCys are antioxidants with anticancer and cancer prevention

properties [15,21–27]. In addition, MeSeCys protects against oxidative stress caused by external oxidants or by γ-radiation [28,29]. It offers selective protection against toxicity and potentiates the antitumor activity of some existing anticancer drugs, including cisplatin [30].

Anticancer drug discovery studies based on the naturally occurring selenium compounds and investigations of their cancer prevention properties have been pursued vigorously during the last three decades [9–16]. However, the anticancer or cancer prevention mechanisms of the selenium compounds are still not known in detail, and they seem to be highly dependent on the speciation of the compounds and the specific metabolic pathways of cell and diseases [14]. The three naturally available compounds SeMet, MeSeCys and selenite appear to be the most important selenium forms in cancer prevention [31,32]. Although SeMet and MeSeCys have similar structures, they display disparate efficacies as anticancer agents [33,34], which is probably related to their

* Corresponding author.

E-mail addresses: liuchunli@uzz.edu.cn (C. Liu), rock@uzz.edu.cn (T. Shi).

different redox properties [14–16]. Significantly, MeSeCys has been found to be not very toxic to the normal human cells, conferring a possibility to achieve a therapeutic selenium window [15].

Reduction of the Pt(IV) anticancer model compounds *trans*-[PtX₂(CN)₄]²⁻ (X = Cl; Br) by SeMet has been characterized kinetically and mechanistically [35]. We here continue these studies with a comparative kinetic analysis on the reduction of the same Pt(IV) model compounds by MeSeCys. There is currently a strong interest in the development of Pt(IV)-based anticancer drugs in order to minimize the toxic effects of the existing platinum-based anticancer drugs and to expand their curing spectra [36]. Our purpose was to implement a detailed kinetic analysis of the redox reactions, to examine the electron transfer mode, to elucidate the reactivity of the MeSeCys species towards reduction of [PtX₂(CN)₄]²⁻, and to compare the reactivity of MeSeCys with that of SeMet studied earlier [35].

2. Experimental section

2.1. Materials

K₂[Pt(CN)₄]·3H₂O and L-norvaline were purchased from Sigma-Aldrich (St. Louis, MO). MeSeCys was obtained from Acros Organics and the good quality was confirmed by its ¹H NMR spectrum (cf. Fig. S1 in Supplementary Data). Acetic acid, sodium acetate, sodium dihydrogen phosphate, disodium hydrogen phosphate, trisodium phosphate, sodium carbonate, sodium bicarbonate, sodium perchlorate, perchloric acid, sodium chloride and sodium bromide, all in analytical grade, were purchased either from Alfa Aesar or from Fisher Scientific and were used for preparation of buffer solutions without further purification. Doubly distilled water was used to prepare all solutions.

K₂[PtCl₂(CN)₄] was synthesized as reported previously [37], except for the final drying step which was done by lyophilization for 24 h, yielding solid K₂[PtCl₂(CN)₄]·½H₂O. Elemental analysis: C, 10.44%, N, 12.18%, H, 0.22%. Found, C, 10.65%, N, 11.58%, H, 0.15%. ¹³C NMR (150 MHz, DMSO d₆): δ 93.2, ¹J¹⁹⁵_{Pt-¹³C} = 837 Hz. K₂[PtBr₂(CN)₄] was prepared according to literature [38], giving rise to solid K₂[PtBr₂(CN)₄]·½H₂O. Elemental analysis: C, 8.80%, N, 10.26%, H, 0.18%. Found, C, 8.65%, N, 9.95%, H, 0.13%. ¹³C NMR (150 MHz, DMSO d₆): δ 90.5, ¹J¹⁹⁵_{Pt-¹³C} = 835 Hz.

2.2. Instrumentation

¹H and ¹³C NMR spectra were recorded by use of a Bruker AVANCE III 600 MHz digital NMR spectrometer (Bruker Daltonics Inc., Billerica, MA, USA). High-resolution mass spectra were recorded on an Apex Ultra 7.0 T FT-ICR mass spectrometer (Bruker Daltonik, Germany) with an electrospray ionization (ESI) of positive mode. An Applied Photophysics SX-20 stopped-flow spectrometer (Applied Photophysics Ltd., Leatherhead, U.K.) was used for recording rapid scan spectra and for kinetic runs. UV–Vis spectra were recorded by use of a TU-1900 spectrophotometer (Beijing Puxi, Inc., Beijing, China) with 1.00 cm quartz cells. The pH values of buffer solutions (for pH > 3) were measured with an Accumet Basic AB15 Plus pH meter equipped with an Accumet combination pH electrode (Fisher Scientific, Pittsburgh, PA). Standard buffers of pH 4.00, 7.00 and 10.00 from Fisher Scientific were used to calibrate the electrode immediately before the pH measurements.

2.3. Reaction media

Buffer solutions containing 2 mM EDTA and 1.0 M ionic strength (μ) were prepared essentially in the same way described earlier [35]. When pH < 3, the reaction media containing 0.10 M NaX (X = Cl and Br) were prepared by combinations of 1.00 M HClO₄, 1.00 M NaClO₄ and 1.00 M NaX. Hydrogen-ion concentrations [H⁺] were obtained from the concentrations of [HClO₄] added; their pH values were calculated using the equation: pH = -log[H⁺] + 0.11, which was based on a mean

activity coefficient of 0.77 in solutions of 1.00 M NaClO₄ [39]. In order to suppress slow hydrolysis of *trans*-[PtX₂(CN)₄]²⁻, 0.10 M NaX was added to all solutions.

2.4. Kinetic measurements

Stock solutions of 1.0 mM *trans*-[PtX₂(CN)₄]²⁻ were prepared by dissolving an appropriate amount of K₂[PtX₂(CN)₄]·½H₂O in solutions containing 0.90 M NaClO₄, 0.09 M NaX and 0.01 M HX; these solutions were wrapped with aluminum foil and kept in a refrigerator. Solutions of Pt(IV) complexes and of MeSeCys for kinetic measurements were prepared, respectively, by adding an appropriate amount of the Pt(IV) stock solution and of MeSeCys to a specific medium. Those solutions were flushed for 10 min with nitrogen before loading onto the stopped-flow instrument and were only used for a couple of hours. Reactions were initiated by mixing equal volumes of Pt(IV) and MeSeCys solutions directly in the stopped-flow spectrometer and were followed under pseudo first-order conditions with MeSeCys in at least 10-fold excess.

2.5. Stoichiometric measurements

Spectrophotometric titration was used to study the reaction stoichiometry as described earlier [40–43]. Briefly, a series of reaction mixtures of *trans*-[PtX₂(CN)₄]²⁻ and MeSeCys were prepared. In these solutions, [Pt(IV)] was maintained constant whereas [MeSeCys] was varied. After a reaction time of about 5 min, the absorbance was measured at 246 nm for the reaction with [PtBr₂(CN)₄]²⁻ and at 255 nm for that with [PtCl₂(CN)₄]²⁻.

3. Results and discussion

3.1. Time-resolved spectra

Rapid scan spectra for the oxidation of MeSeCys by [PtBr₂(CN)₄]²⁻ in acidic medium as recorded by the stopped-flow spectrometer are displayed in Fig. 1. Two clear isosbestic points at 276.7 and 286.1 nm are observable. For the oxidation of MeSeCys by [PtCl₂(CN)₄]²⁻, the rapid scan spectra recorded in a phosphate buffer of pH 7.35 are given

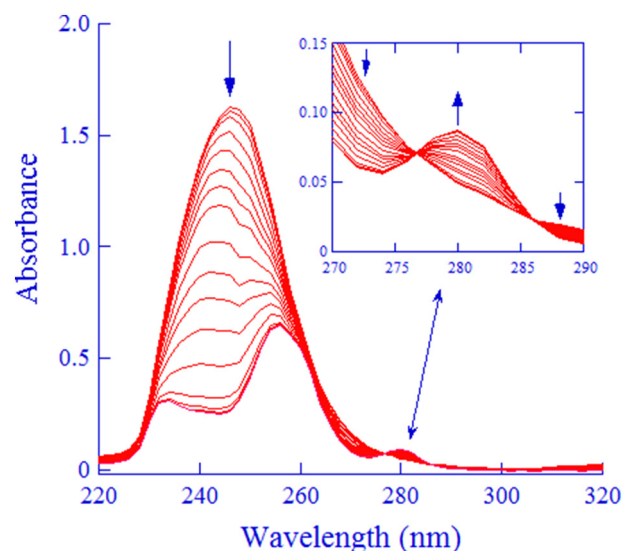


Fig. 1. Rapid scan spectra for the reaction between *trans*-[PtBr₂(CN)₄]²⁻ and MeSeCys under the reaction conditions: [Pt(IV)] = 0.06 mM, [MeSeCys] = 1.0 mM; reaction medium: [HClO₄] = 0.10 M, [Br⁻] = 0.10 M, and μ = 1.0 M; temperature: 25.0 °C. The spectra were obtained at 3, 6, 10, 20, 30, 40, 50, 60, 80, 100, 120, 150, 200, 300, 400, and 500 ms. Insert: The spectra were shown at enlarged scale to display the isosbestic points at 276.7 and 286.1 nm.

in Fig. S2 in Supplementary Data. These spectra also display two well-defined isosbestic points at 244.2 and 286.1 nm (cf. Fig. S3 in Supplementary Data). The sharp isosbestic points in both cases indicate that the reduction of $[\text{PtX}_2(\text{CN})_4]^{2-}$ to $[\text{Pt}(\text{CN})_4]^{2-}$ is a simple process involving a direct conversion of $[\text{PtX}_2(\text{CN})_4]^{2-}$ to $[\text{Pt}(\text{CN})_4]^{2-}$. The contribution from an absorbance change produced by the MeSeCys oxidation to the overall spectral changes does not influence the sharpness of the isosbestic points. The well-defined isosbestic points exclude the formation of any intermediate species via a substitution of halide in $[\text{PtX}_2(\text{CN})_4]^{2-}$ by MeSeCys, which is also in agreement with the general substitution inertness of Pt(IV) complexes.

3.2. Overall second-order kinetics

Under pseudo first-order conditions with $[\text{MeSeCys}] \geq 10 \cdot [\text{Pt(IV)}]$, kinetic traces recorded between 240 and 246 nm for the $[\text{PtBr}_2(\text{CN})_4]^{2-}$ reaction and at 255 nm for the $[\text{PtCl}_2(\text{CN})_4]^{2-}$ reaction were well simulated by single exponentials indicating that the redox reactions are indeed first-order in $[\text{Pt(IV)}]$. The effect of added $[\text{Cl}^-]$ on the reduction rate in the case of $[\text{PtCl}_2(\text{CN})_4]^{2-}$ was examined in the region $1.0 \text{ mM} \leq [\text{Cl}^-] \leq 100 \text{ mM}$. The k_{obsd} values as a function of $[\text{Cl}^-]$ are listed in Table S1 in Supplementary Data. The change of $[\text{Cl}^-]$ did not affect the k_{obsd} values.

Pseudo first-order rate constants, k_{obsd} , as functions of $[\text{MeSeCys}]$ and of pH were collected extensively. In the case of $[\text{PtCl}_2(\text{CN})_4]^{2-}$, k_{obsd} values were measured in the pH range of 0.41 to 10.36. For

$[\text{PtBr}_2(\text{CN})_4]^{2-}$, the reaction was only investigated between pH 0.41 and 5.12 since the bromide complex is not stable in neutral and basic media [38]. Plots of k_{obsd} versus $[\text{MeSeCys}]$ are linear and passing through the origin (cf. Figs. 2 and 3), demonstrating that the reduction is also first-order in $[\text{MeSeCys}]$. Eq. (1) expresses the overall second-order kinetics, where k' denotes the observed second-order rate constants.

$$-d[\text{Pt(IV)}]/dt = d[\text{Pt(II)}]/dt = k_{\text{obsd}}[\text{Pt(IV)}] = k'[\text{MeSeCys}][\text{Pt(IV)}] \quad (1)$$

The variation of k' with pH is summarized in Table S2 in Supplementary Data.

3.3. Reaction stoichiometry and product identification

For the reaction of $[\text{PtBr}_2(\text{CN})_4]^{2-}$, the spectrophotometric titration was studied in a medium of 0.10 M HClO_4 ; a plot of the absorbance at 246 nm as a function of $[\text{MeSeCys}]$ is shown in Fig. 4. The data points follow two crossing straight lines and the intersection point renders a ratio $[\text{Pt(IV)}]:[\text{MeSeCys}] = 0.060 \text{ mM} : (0.057 \pm 0.02) \text{ mM} = 1 : (0.95 \pm 0.04)$. Fig. S4 in Supplementary Data displays the corresponding plot of the absorbance at 255 nm in the case $[\text{PtCl}_2(\text{CN})_4]^{2-}$, giving similarly an intersection and a ratio of $[\text{Pt(IV)}]:[\text{MeSeCys}] = 1 : (1.02 \pm 0.05)$. Hence, the obtained $[\text{Pt(IV)}]:[\text{MeSeCys}]$ ratios for both $[\text{PtBr}_2(\text{CN})_4]^{2-}$ and $[\text{PtCl}_2(\text{CN})_4]^{2-}$ impart a 1:1 stoichiometry within experimental errors. Moreover, in blank experiments using L-norvaline to replace

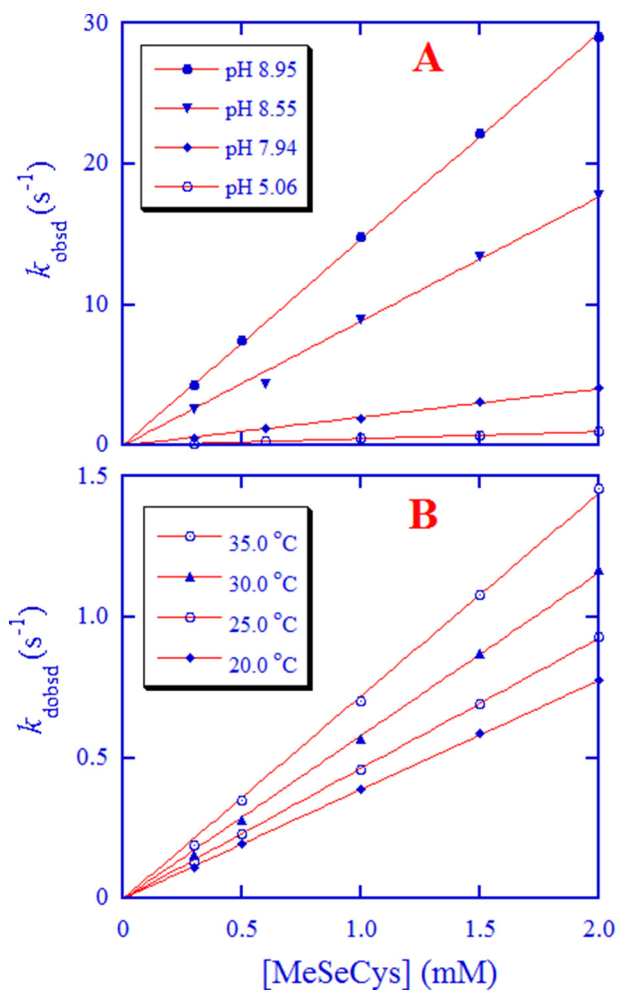


Fig. 2. Plots of k_{obsd} versus $[\text{MeSeCys}]$ for the reduction of $[\text{PtCl}_2(\text{CN})_4]^{2-}$ by MeSeCys at $\mu = 1.0 \text{ M}$. (A) In various pH buffers at 25.0 °C. (B) At several temperatures in a buffer of pH 4.43.

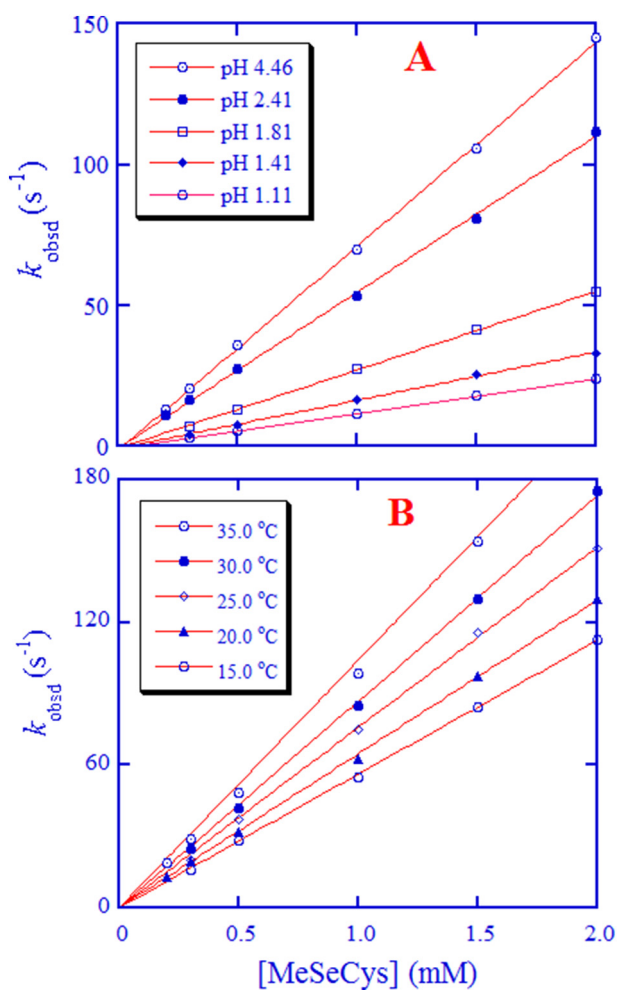


Fig. 3. Plots of k_{obsd} versus $[\text{MeSeCys}]$ for the reduction of $[\text{PtBr}_2(\text{CN})_4]^{2-}$ by MeSeCys at $\mu = 1.0 \text{ M}$. (A) In various pH buffers at 25.0 °C. (B) At several temperatures in a buffer of pH 4.01.

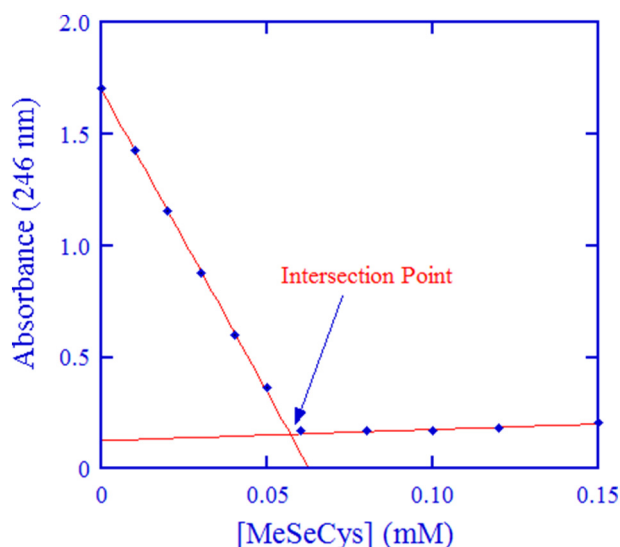
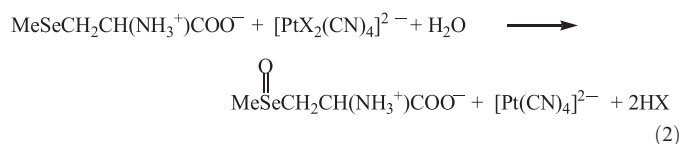


Fig. 4. Spectrophotometric titration: absorbance at 246 nm for a series of reaction mixtures of $[\text{PtBr}_2(\text{CN})_4]^{2-}$ with MeSeCys in which [MeSeCys] was varied from 0 to 0.15 mM and $[\text{Pt}(\text{IV})] = 0.060$ mM was kept constant. Reaction medium: $[\text{H}^+] = 0.10$ M, $[\text{Br}^-] = 0.10$ M, and $\mu = 1.0$ M. Reaction time: about 5 min at room temperature.

MeSeCys (thus using a methylene group to replace the selenium in MeSeCys), no reaction was observed between $[\text{PtX}_2(\text{CN})_4]^{2-}$ and L-norvaline, showing that the observed redox reactions take place via the selenium atom. Consequently, the 1:1 stoichiometry suggests that MeSeCys is oxidized to its selenoxide form according to Eq. (2):



SeMet is often oxidized to its selenoxide form by various oxidants [35,44–46]. In the case of MeSeCys, the oxidation product has been less extensively characterized. Therefore, high resolution mass spectra

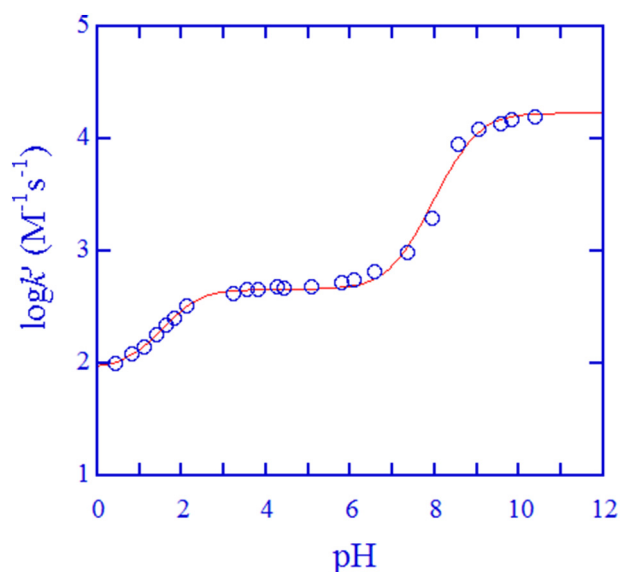


Fig. 5. Second-order rate constants k' (in logarithmic scale) as a function of pH at 25.0 °C and $\mu = 1.0$ M (data points) for the reduction of $[\text{PtCl}_2(\text{CN})_4]^{2-}$ by MeSeCys. The solid curve was produced from the best fit of Eq. (3) to the experimental data by a weighted nonlinear least-squares routine.

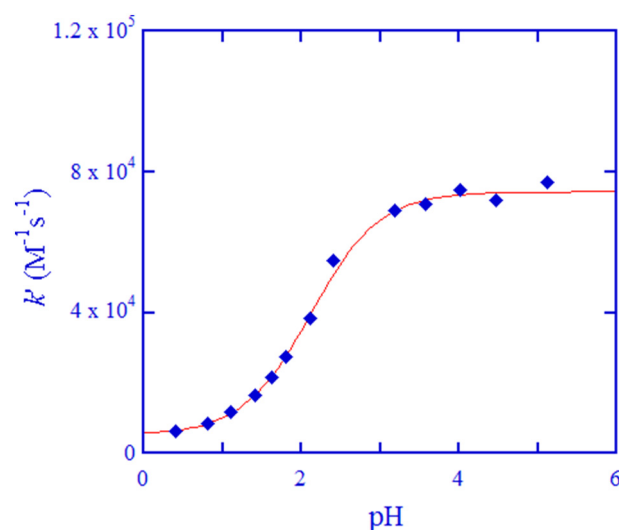


Fig. 6. Second-order rate constants k' as a function of pH at 25.0 °C and $\mu = 1.0$ M (data points) for the reduction of $[\text{PtBr}_2(\text{CN})_4]^{2-}$ by MeSeCys. The solid curve represents the best fit of Eq. (4) to the experimental data by a weighted nonlinear least-squares routine.

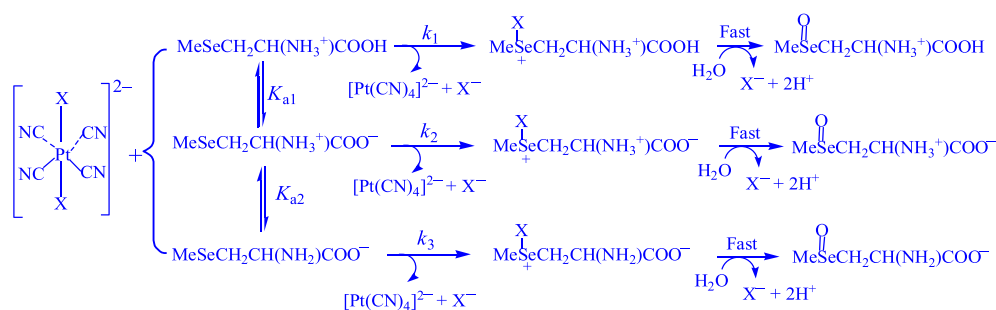
were recorded for two samples: one was 1.0 mM MeSeCys in 10 mM HCl and the other one was a reaction mixture of 1.0 mM MeSeCys and 1.2 mM *trans*- $[\text{PtCl}_2(\text{CN})_4]^{2-}$ in 10 mM HCl. The mass spectra are displayed in Fig. S5 in Supplementary Data; the peak assignments are given in the figure legend. MeSeCys selenoxide and largely in its hydrate form $\text{MeSe}(\text{OH})_2\text{Cys}$ (cf. its structure and its formation in the legend of Fig. S5 in Supplementary Data [46]) are confirmed by the mass spectra. $\text{MeSe}(\text{OH})_2\text{Cys}$ is expected to be formed after the rate-determining-steps. Therefore, Eq. (2) is justified by the mass spectral analysis.

3.4. Reaction mechanism

The reaction parameters deduced for the present reaction systems, including the rapid scan spectra, the overall second-order kinetics, the k' versus pH profiles in Figs. 5 and 6, and the 1:1 redox stoichiometry are similar to those observed in the reduction of $[\text{PtX}_2(\text{CN})_4]^{2-}$ by SeMet [35]. Therefore, a similar reaction mechanism, as the one depicted in Scheme 1, is anticipated for the present reaction systems also. The rate-determining reactions (denoted by $k_1 - k_3$) proceed via inner-sphere electron transfer mechanisms, leading to an X^+ transfer from the Pt(IV) complexes to the attacking selenium atom (cf. further discussion below). Eq. (3) will be the rate expression for k' derived from Scheme 1, where K_{a1} and K_{a2} are the protolysis constants of MeSeCys, and a_{H} pertains to the proton activity, corresponding exactly to the measured pH values.

$$k' = \frac{k_1 a_{\text{H}}^2 + k_2 K_{a1} a_{\text{H}} + k_3 K_{a1} K_{a2}}{a_{\text{H}}^2 + K_{a1} a_{\text{H}} + K_{a1} K_{a2}} \quad (3)$$

By use of a weighted non-linear least-squares method, Eq. (3) was employed to simulate the $k' - \text{pH}$ dependence data in Fig. 5 for the reduction of the chloride complex, with $k_1 - k_3$ and K_{a1} and K_{a2} all as tunable parameters. No well defined pK_a values at 25.0 °C and 1.0 M ionic strength are available in the literature, only approximate values at undefined temperature and ionic strength ($\text{pK}_{a1} \sim 2$ and $\text{pK}_{a2} = 8.8$) were found [47]. The resulting good fit shown in Fig. 5 not only justifies the conformity of Eq. (3) to the $k' - \text{pH}$ data but also affords well-defined pK_a -values ($\text{pK}_{a1} = 1.90 \pm 0.15$ and $\text{pK}_{a2} = 8.74 \pm 0.09$) and the $k_1 - k_3$ values listed in Table 1. The ratios $k_2/k_1 = 9$ and $k_3/k_2 = 37$ referring to the deprotonations of the $-\text{COOH}$ and $-\text{NH}_3^+$ groups in MeSeCys, respectively, confer very significant reactivity differences between the three protolytic species.



For X = Cl, Pt(IV) = *trans*-[PtCl₂(CN)₄]²⁻; for X = Br, Pt(IV) = *trans*-[PtBr₂(CN)₄]²⁻

Scheme 1. Reaction mechanism proposed for the redox reactions between *trans*-[PtX₂(CN)₄]²⁻ and MeSeCys.

The data in Fig. 6 refer to reduction of the bromide complex. It only involves the deprotonation of the carboxylic group in MeSeCys, since [PtBr₂(CN)₄]²⁻ is only stable in acidic media, precluding kinetic data collection in neutral and basic media [38]. Accordingly, Eq. (3) is simplified to Eq. (4):

$$k' = (k_1 a_H + k_2 K_{a1}) / (a_H + K_{a1}) \quad (4)$$

Eq. (4) was used to simulate the k' – pH dependence data given in Fig. 6. It also results in a good fit and provides $pK_{a1} = 2.12 \pm 0.15$ and the values of k_1 and k_2 listed in Table 1. The agreement between the pK_{a1} values derived for the two Pt(IV) reactions is good within experimental errors.

3.5. Activation parameters

The species distribution diagram of MeSeCys *versus* pH was calculated by use of the pK_a values derived here; in addition, the reactivity *versus* pH distribution diagram for the MeSeCys species was computed for the reaction of [PtCl₂(CN)₄]²⁻ with MeSeCys utilizing the pK_a values and the rate constants k_1 – k_3 (cf. the diagrams in Fig. S6 in Supplementary Data) [40,42]. The diagrams show that in the region $3.5 < \text{pH} < 5$, the zwitterionic form of MeSeCys (MeSeCH₂CH(NH₃⁺)CO₂⁻) is the only species contributing both to the total population and to the total reactivity. Therefore, k' equals k_2 in Scheme 1 in this region. Temperature dependencies of k_{obsd} in buffers of this region are shown in Fig. 2 for the reaction of [PtCl₂(CN)₄]²⁻ and in Fig. 3 for the reaction of [PtBr₂(CN)₄]²⁻, respectively. Table 2 summarizes the k_2 values at different temperatures. Activation parameters were evaluated from the perfectly linear Eyring plots (Fig. S7 in Supplementary Data), and are also given in Table 2.

Table 1

Second-order rate constants for reduction of *trans*-[PtX₂(CN)₄]²⁻ (X = Cl and Br) by the protolytic species of MeSeCys and MeSeMet at 25.0 °C and $\mu = 1.0$ M; cf. Scheme 1.

[PtX ₂ (CN) ₄] ²⁻	Species	k_m	Value/M ⁻¹ s ⁻¹	Ref.
X = Cl	from MeSeCys:			
	MeSeCH ₂ CH(NH ₃ ⁺)CO ₂ H	k_1	90 ± 5	this work
	MeSeCH ₂ CH(NH ₃ ⁺)CO ₂ ⁻	k_2	458 ± 9	this work
X = Br	MeSeCH ₂ CH(NH ₂)CO ₂ ⁻	k_3	$(1.69 \pm 0.08) \times 10^4$	this work
	MeSeCH ₂ CH(NH ₃ ⁺)CO ₂ H	k_1	$(5.3 \pm 0.2) \times 10^3$	this work
	MeSeCH ₂ CH(NH ₃ ⁺)CO ₂ ⁻	k_2	$(7.4 \pm 0.2) \times 10^4$	this work
X = Cl	from SeMet:			
	MeSe(CH ₂) ₂ CH(NH ₃ ⁺)CO ₂ H	k_1	$(1.18 \pm 0.02) \times 10^4$	[35]
	MeSe(CH ₂) ₂ CH(NH ₃ ⁺)CO ₂ ⁻	k_2	$(1.65 \pm 0.03) \times 10^4$	[35]
X = Br	MeSe(CH ₂) ₂ CH(NH ₂)CO ₂ ⁻	k_3	$(6.6 \pm 0.2) \times 10^4$	[35]
	MeSe(CH ₂) ₂ CH(NH ₃ ⁺)CO ₂ H	k_1	$(8.7 \pm 0.2) \times 10^5$	[35]
	MeSe(CH ₂) ₂ CH(NH ₃ ⁺)CO ₂ ⁻	k_2	$(2.1 \pm 0.1) \times 10^6$	[35]

3.6. Bridged two-electron transfer mode

The rate-determining steps of the reductive elimination reactions of *trans*-dihalo-Pt(IV) complexes have been interpreted to take place through an inner-sphere electron transfer, *via* a bridge formation between one of the axially coordinated halides of the platinum complexes and the attacking selenium atom of the reductants [35,40,48]. This mode of two-electron transfer predicts that a good bridging atom should favor the electron transfer. The derived rate constants in Table 1 for MeSeCys clearly indicate that the reduction of [PtBr₂(CN)₄]²⁻ is much faster than that of [PtCl₂(CN)₄]²⁻ (54–148 times). Similar rate enhancements were observed when SeMet was used as the reductant (Table 1). These rate enhancements could be due to the better bridging effect of the coordinated bromide compared to its chloride counterpart in the Pt(IV) complexes.

The relatively large negative and virtually equal values of the activation entropies (Table 2) obtained for [PtCl₂(CN)₄]²⁻ and [PtBr₂(CN)₄]²⁻ suggest a compact structure of the transition state, which is in line with the nature of second-order kinetics. However, the reduction of [PtBr₂(CN)₄]²⁻ proceeds with a significantly smaller activation enthalpy than that of [PtCl₂(CN)₄]²⁻ due to the better bridging effect of coordinated bromide, this in spite of the fact that [PtBr₂(CN)₄]²⁻/[Pt(CN)₄]²⁻ ($E^\circ = 0.75$ V [49]) has a lower redox potential than [PtCl₂(CN)₄]²⁻/[Pt(CN)₄]²⁻ ($E^\circ = 0.89$ V [50]). Thus, the obtained activation parameters strongly support the bridged electron transfer mode. To the best of our knowledge, this work, together with a previous one [35], shows for the first time that an X⁺ transfer from the oxidants to the selenium-containing compounds takes place.

3.7. Comparison of rate constants

Selenium compounds are often characterized by their strong antioxidant properties, which is linked essentially to their major biological roles [5,51–53]. The reactivity of SeMet and MeSeCys in reducing some oxidants encountered in human bodies has been studied, including hydroxyl radicals ($\bullet\text{OH}$) [47], chlorine radicals ($\bullet\text{Cl}_2^-$) [47] and

Table 2

Rate constants and activation parameters for reduction of *trans*-[PtX₂(CN)₄]²⁻ by the zwitterionic form of MeSeCys (MeSeCH₂CH(NH₃⁺)CO₂⁻) at $\mu = 1.0$ M.

Pt(IV)	$t/^\circ\text{C}$	$k_2/\text{M}^{-1} \text{s}^{-1}$	$\Delta H^\ddagger/\text{kJ}\cdot\text{mol}^{-1}$	$\Delta S^\ddagger/\text{J}\cdot\text{K}^{-1}\cdot\text{mol}^{-1}$
[PtCl ₂ (CN) ₄] ²⁻	20.0	388 ± 9	28.8 ± 1.8	-92 ± 10
	25.0	463 ± 15		
	30.0	580 ± 19		
	35.0	721 ± 25		
[PtBr ₂ (CN) ₄] ²⁻	15.0	$(5.6 \pm 0.1) \times 10^4$	20.3 ± 1.3	-83 ± 8
	20.0	$(6.4 \pm 0.1) \times 10^4$		
	25.0	$(8.7 \pm 0.1) \times 10^4$		
	30.0	$(1.04 \pm 0.02) \times 10^5$		

hypothiocyanous acid (HOSCN) [51]. The reactivity ratios $k'(\text{SeMet})/k'(\text{MetSeCys})$ were found to be 0.9 for $\bullet\text{OH}$ at pH 1, 1.6 for $\bullet\text{Cl}_2^-$ at pH 1, and ≥ 6 for HOSCN at pH 7.4; the ratios for $\bullet\text{OH}$ and $\bullet\text{Cl}_2^-$ might be less accurate since the rate constants are close to the diffusion controlled ones.

The relative values of k_1 , k_2 and k_3 for MeSeCys show that the rates increase significantly as the charge becomes more negative, since in the rate-determining steps, the selenium atom is accommodating the positively charged X^+ . The trend becomes less pronounced in the case of SeMet where the charge effects are attenuated by the additional methylene group inserted between the Se atom and the charges. A comparison between the rate constants in Table 1 shows that the reactivity of SeMet and MeSeCys towards reduction of $[\text{PtX}_2(\text{CN})_4]^{2-}$ are largely different. Moreover, the difference is species dependent: $k_1(\text{SeMet})/k_1(\text{MetSeCys}) = 128$, $k_2(\text{SeMet})/k_2(\text{MetSeCys}) = 35$, and $k_3(\text{SeMet})/k_3(\text{MetSeCys}) = 4$ for $[\text{PtCl}_2(\text{CN})_4]^{2-}$; and $k_1(\text{SeMet})/k_1(\text{MetSeCys}) = 174$, $k_2(\text{SeMet})/k_2(\text{MetSeCys}) = 30$ for $[\text{PtBr}_2(\text{CN})_4]^{2-}$. The reactivity differences observed in the present work are significantly larger than those found above, indicating the variable reactivity of SeMet and MeSeCys towards reduction of different oxidants. Those reactivity differences might be related to their disparate efficacies as anticancer agents [33,34].

3.8. Concluding remarks

The reduction of $[\text{PtX}_2(\text{CN})_4]^{2-}$ by MeSeCys was analyzed kinetically and mechanistically in a broad pH range by use of rapid scan, stopped-flow and high resolution mass spectral techniques. The rate-determining steps are rationalized in terms of bridged two-electron transfer and the rate constants for those steps have been evaluated. In the reduction of $[\text{PtX}_2(\text{CN})_4]^{2-}$, MeSeCys and SeMet show similar kinetic and mechanistic characters, but there is a big reactivity difference. The difference is not only the largest one observed so far, but it is also dependent on the protolytic species of MeSeCys and SeMet. The reactivity difference observed here might be one reason for the different efficacies of these two selenium compounds as anticancer agents. Moreover, this kinetic analysis also offers novel values for the $\text{p}K_a$ values of MeSeCys at 25.0 °C and 1.0 M ionic strength.

Acknowledgements

Financial support of this work by a set-up fund from Zaozhuang University (1020717) is gratefully acknowledged. L.I.E. thanks the Royal Physiographic Society of Lund for support. We thank one of the reviewers who gave some thoughtful suggestions for revision of the manuscript.

Appendix A. Supplementary data

Supplementary data to this article can be found online at <https://doi.org/10.1016/j.molliq.2018.09.056>.

References

- [1] U. Tinggi, Environ. Health Prev. Med. 13 (2008) 102–108.
- [2] L.V. Papp, A. Holmgren, K.K. Khanna, Antioxid. Redox Signal. 12 (2010) 793–795.
- [3] Z. Huang, A.H. Rose, P.R. Hoffmann, Antioxid. Redox Signal. 16 (2012) 705–743.
- [4] C. Benstoem, A. Goetzenich, S. Kraemer, S. Borosch, W. Manzanarez, G. Hardy, C. Stoppe, Nutrients 7 (2015) 3094–3118.
- [5] Y. Mehdi, J.-L. Hornick, L. Istasse, I. Dufrasne, Molecules 18 (2013) 3292–3311.
- [6] M. Roman, P. Jitaru, C. Barbante, Metallomics 6 (2014) 25–54.
- [7] J.K. Wrobel, R. Power, M. Toborek, IUBMB Life 68 (2016) 97–105.
- [8] H.E. Ganther, Carcinogenesis 20 (1999) 1657–1666.
- [9] Y.S. Kim, J. Milner, Nutr. Cancer 40 (2001) 50–54.
- [10] L. Patrick, Altern. Med. Rev. 9 (2004) 239–258.
- [11] M.I. Jackson, G.F. Combs Jr., Curr. Opin. Clin. Nutr. Metab. Care 11 (2008) 718–726.
- [12] J. Brozmanová, D. Maniková, V. Vičková, M. Chovanec, Arch. Toxicol. 84 (2010) 919–938.
- [13] Y.C. Chen, K.S. Prabhu, A.M. Mastro, Nutrients 5 (2013) 1149–1168.
- [14] A.P. Fernandes, V. Gandin, Biochim. Biophys. Acta 1850 (2015) 1642–1660.
- [15] S. Misra, M. Boylan, A. Selvam, J.E. Spallholz, M. Björnstedt, Nutrients 7 (2015) 3536–3556.
- [16] M. Álvarez-Pérez, W. Ali, M.A. Marć, J. Hanzlik, E. Dominguez-Álvarez, Molecules 23 (2018) 628.
- [17] S.J. Fairweather-Tait, R. Collings, R. Hurst, Am. J. Clin. Nutr. 91 (2010) 1484S–1491S.
- [18] Z. Pedrero, Y. Madrid, Anal. Chim. Acta 634 (2009) 135–152.
- [19] H. Yang, X. Jia, Regul. Toxicol. Pharmacol. 70 (2014) 720–727.
- [20] M.P. Rayman, Lancet 379 (2012) 1256–1268.
- [21] D. Medina, H. Thompson, H. Ganther, C. Ip, Nutr. Cancer 40 (2001) 12–17.
- [22] R. Sinha, D. Medina, Carcinogenesis 18 (1997) 1541–1547.
- [23] A. Bhattacharya, Expert Opin. Drug Deliv. 8 (2011) 749–763.
- [24] Z. Li, L. Carrier, A. Belame, A. Thiagarajah, V.A. Salvo, M.E. Burrow, B.G. Rowan, Breast Cancer Res. Treat. 118 (2009) 33–43.
- [25] Y. Liu, X. Liu, Y. Guo, Z. Liang, Y. Tian, L. Lu, X. Zhao, Y. Sun, X. Zhao, H. Zhang, Y. Dong, Prostate 75 (2015) 1001–1008.
- [26] G. Huang, B.C. Yong, M.H. Xu, J.C. Li, H.H. Guo, J.N. Shen, Nutr. Cancer 67 (2015) 847–856.
- [27] J.K. Yeo, S.D. Cha, C.H. Cho, S.P. Kim, J.W. Cho, W.K. Baek, M.H. Suh, T.K. Kwon, J.W. Park, S.I. Suh, Cancer Lett. 182 (2002) 83–92.
- [28] S. Cuello, S. Ramos, R. Mateos, M.A. Martín, Y. Madrid, C. Camara, L. Bravo, L. Goya, Anal. Bioanal. Chem. 389 (2007) 2167–2178.
- [29] H.S. Shin, W.J. Yang, E.M. Choi, J. Trace Elem. Med. Biol. 27 (2013) 154–159.
- [30] S. Cao, F.A. Durrani, K. Toth, Y.M. Rustum, Br. J. Cancer 110 (2014) 1733–1743.
- [31] K. Stokel, Selenium: which forms protect against cancer? Life Extension Magazine, 2012, Ref. <http://www.lifeextension.com/magazine/2012/ss/selenium-protect-against-cancer/page-01>.
- [32] D.R. Ellis, T.G. Sors, D.G. Brunk, G. Albrecht, C. Orser, B. Lahner, K.V. Wood, H.H. Harris, I.J. Pickering, D.E. Salt, BMC Plant Biol. 4 (2004) 1.
- [33] L.M. Weekley, J.B. Aitken, S. Vogt, L.A. Finney, D.J. Paterson, M.D. de Jonge, D.L. Howard, I.F. Musgrave, H.H. Harris, Biochemistry 50 (2011) 1641–1650.
- [34] C.M. Weekley, J.B. Aitken, I.F. Musgrave, H.H. Harris, Biochemistry 51 (2012) 736–738.
- [35] S. Huo, J. Dong, S. Shen, Y. Ren, C. Song, J. Xu, T. Shi, Dalton Trans. 43 (2014) 15328–15336.
- [36] X. Han, J. Sun, Y. Wang, Z. He, Med. Res. Rev. 35 (2015) 1268–1299.
- [37] T. Shi, L.I. Elding, Inorg. Chim. Acta 282 (1998) 55–60.
- [38] C.E. Skinner, M.M. Jones, J. Am. Chem. Soc. 91 (1969) 1984–1990.
- [39] M. Kimura, M. Yamamoto, S. Yamabe, J. Chem. Soc. Dalton Trans. (1982) 423–427.
- [40] J. Dong, Y. Ren, S. Huo, S. Shen, J. Xu, H. Tian, T. Shi, Dalton Trans. 45 (2016) 11326–11337.
- [41] C. Nan, J. Dong, X. Jiao, H. Shi, J. Duan, T. Shi, Transit. Met. Chem. 42 (2017) 9–15.
- [42] J. Dong, Y. Ren, S. Sun, J. Yang, C. Nan, H. Shi, J. Xu, J. Duan, T. Shi, L.I. Elding, Dalton Trans. 46 (2017) 8377–8386.
- [43] C. Nan, J. Dong, H. Tian, H. Shi, S. Shen, J. Xu, X. Li, T. Shi, J. Mol. Liq. 256 (2018) 489–496.
- [44] A.A. Isab, Inorg. Chim. Acta 80 (1983) L3–L4.
- [45] S. Padmaja, G.L. Squadrito, J.-N. Lemerrier, R. Cueto, W.A. Pryor, Free Radic. Biol. Med. 21 (1996) 317–322.
- [46] R.J. Krause, S.C. Glocke, A.R. Sicuri, S.L. Ripp, A.A. Elfarra, Chem. Res. Toxicol. 19 (2006) 1643–1649.
- [47] B. Mishra, K.I. Priyadarsini, H. Mohan, J. Phys. Chem. A 110 (2006) 1894–1900.
- [48] J. Dong, H. Tian, C. Song, T. Shi, L.I. Elding, Dalton Trans. 47 (2018) 5548–5552.
- [49] K.A. Morgan, M.M. Jones, J. Inorg. Nucl. Chem. 34 (1972) 275–296.
- [50] R.N. Goldberg, L.G. Helper, Chem. Rev. 68 (1968) 229–252.
- [51] O. Skaff, D.I. Pattison, P.E. Morgan, R. Bachana, V.K. Jain, I. Priyadarsini, M.J. Davies, Biochem. J. 441 (2012) 305–316.
- [52] A.S. Rahmanto, M.J. Davies, IUBMB Life 64 (2012) 863–871.
- [53] H.J. Reich, R.J. Hondal, ACS Chem. Biol. 11 (2016) 821–841.